



# Mutations in the *Drosophila* tricellular junction protein M6 synergize with *Ras*<sup>V12</sup> to induce apical cell delamination and invasion

Brandon S. Dunn<sup>a,b</sup>, Lindsay Rush<sup>a,b</sup>, Jin-Yu Lu<sup>a,b</sup>, and Tian Xu<sup>a,b,c,d,1</sup>

<sup>a</sup>Howard Hughes Medical Institute, Yale University School of Medicine, New Haven, CT 06510; <sup>b</sup>Department of Genetics, Yale University School of Medicine, New Haven, CT 06510; <sup>c</sup>State Key Laboratory of Genetic Engineering, School of Life Sciences, Fudan University, 200433 Shanghai, China; and <sup>d</sup>National Center for International Research, Fudan–Yale Biomedical Research Center, Institute of Developmental Biology and Molecular Medicine, School of Life Sciences, Fudan University, 200433 Shanghai, China

Edited by Norbert Perrimon, Harvard Medical School, Boston, MA, and approved June 15, 2018 (received for review May 1, 2018)

Complications from metastasis are responsible for the majority of cancer-related deaths. Despite the outsized medical impact of metastasis, remarkably little is known about one of the key early steps of metastasis: departure of a tumor cell from its originating tissue. It is well documented that cellular delamination in the basal direction can induce invasive behaviors, but it remains unknown if apical cell delamination can induce migration and invasion in a cancer context. To explore this feature of cancer progression, we performed a genetic screen in *Drosophila* and discovered that mutations in the protein M6 synergize with oncogenic Ras to drive invasion following apical delamination without crossing a basement membrane. Mechanistically, we observed that M6-deficient *Ras*<sup>V12</sup> clones delaminate as a result of alterations in a Cane-RhoA-myosin II axis that is necessary for both the delamination and invasion phenotypes. To uncover the cellular roles of M6, we show that it localizes to tricellular junctions in epithelial tissues where it is necessary for the structural integrity of multicellular contacts. This work provides evidence that apical delamination can precede invasion and highlights the important role that tricellular junction integrity can play in this process.

tricellular junctions | cell delamination | *Drosophila* | cancer | invasion

Cells are known to delaminate from their tissues in both the apical and basal directions during development and in disease conditions (1–3). Importantly, cell delamination plays a vital role in cancer progression as it is one way that a cancer cell can escape its originating tissue before spreading to more distant sites (4). During tumor progression, different models have revealed that cell delamination in the apical direction can lead either to the elimination of the delaminated cells (5–7) or to the overgrowth of those cells (8–10). However, invasive behaviors have not been observed to follow apical delamination but instead have been shown to occur only through basal delamination (5, 7, 11–13).

During basal delamination-induced invasion, basement membrane degradation and cell invasion into the underlying tissue can be observed in fixed tissues. On the other hand, if cancer cells leave the tissue by migrating and invading following apical delamination, the invasion would not leave such a histologically visible trail as this invasion could occur without crossing the basement membrane but instead through migration along connected tissues. As such, alternate methods in a suitable system would be needed to recognize if apical delamination is able to induce invasion. Thus, although previous work has documented direct basal delamination and invasion during metastasis in animal models and human patients, it does not preclude the possibility that invasion can be initiated by apical delamination as well. *Drosophila* cancer models are well suited to address the role of apical delamination in inducing invasive behaviors due to their simple tissue architecture that allows for the easy identification of an apical delamination event, as well as established techniques to image intact living tissues over time to follow the fates of

apically delaminated cells. Here we document that cell migration and invasion can be induced via apical delamination through the characterization of a tumor suppressor, M6, in *Drosophila*.

## Results

**M6 Mutations Cooperate with *Ras*<sup>V12</sup> to Drive Tumor Progression.** To gain a deeper understanding into the mechanisms of cancer progression, we performed an ethyl methanesulfonate screen for mutations that can induce overgrowth and invasion of otherwise benign *Ras*<sup>V12</sup> eye-disk clones. From this screen, we identified a complementation group of three alleles that deficiency mapping and complementation testing with a preexisting *P*-element insertion line pinpointed to contain mutations in the tetraspan gene M6 (Fig. 1A) (14, 15). Animals either homozygous for the weak alleles (*M6*<sup>G152E</sup>, *M6*<sup>NC</sup>, and *M6*<sup>P</sup>) or transheterozygous over deficiency [*M6*<sup>G152E/Df(3L)BSC418</sup>] are larval-lethal with an extended larval stage (SI Appendix, Fig. S1K). Imaginal discs from these larvae are overgrown and exhibit ectopic folds, which identifies M6 as a tumor suppressor (SI Appendix, Fig. S1A–J). Animals homozygous for the strong mutation (*M6*<sup>W186\*</sup>) or transheterozygous over deficiency are embryonic-lethal, suggesting that it is a null allele. Indeed, DNA sequencing revealed that the *M6*<sup>W186\*</sup> allele has a premature stop codon at amino acid position 186 in the third transmembrane domain, which truncates more than 40% of the protein (referred to as *M6*<sup>−/−</sup> in the following analysis), while the *M6*<sup>G152E</sup> allele has a missense mutation (SI Appendix, Fig. S1L).

## Significance

Complications from metastasis are responsible for the majority of cancer-related deaths, yet we understand relatively little about how cells initiate metastasis and depart from their original tissues. To uncover the cellular and molecular mechanisms governing departure of a tumor cell from its tissue, we show here that, in a *Drosophila* cancer model, invasion can be initiated through apical delamination. Furthermore, this apical delamination occurs as a result of alterations in the junctions between three neighboring cells, termed “tricellular junctions.” This work provides evidence that apical delamination can initiate invasion in certain contexts and highlights the important role that tricellular junction integrity can play in this process.

Author contributions: B.S.D., L.R., and T.X. designed research; B.S.D., L.R., and J.-Y.L. performed research; B.S.D., L.R., and T.X. analyzed data; and B.S.D. and T.X. wrote the paper.

The authors declare no conflict of interest.

This article is a PNAS Direct Submission.

Published under the PNAS license.

<sup>1</sup>To whom correspondence should be addressed. Email: tian.xu@yale.edu.

This article contains supporting information online at [www.pnas.org/lookup/suppl/doi:10.1073/pnas.1807343115/-DCSupplemental](http://www.pnas.org/lookup/suppl/doi:10.1073/pnas.1807343115/-DCSupplemental).

Published online July 30, 2018.

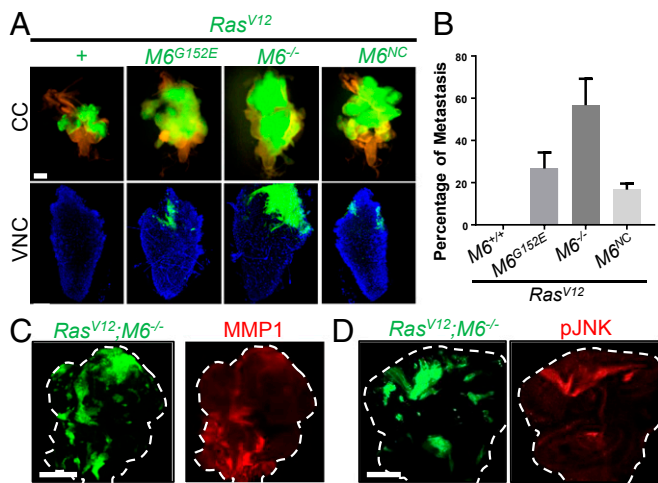


**Fig. 1.** Mutations in M6 induce invasion of  $Ras^{V12}$  clones. (A) Clones (GFP labeled) of the indicated genotypes were fixed in the cephalic complex (CC, *Top*) to show overall clone size and in the VNC (*Bottom*) to show invasion ( $n > 150$  of each genotype). M6<sup>-/-</sup> notation refers to the M6<sup>W186\*</sup> allele. (Scale bar: *Top*, 200  $\mu$ m; *Bottom*, 50  $\mu$ m.) (B) Quantification of the percentage of larvae that show invasion into the VNC. Three biological replicates of 50 larvae for each genotype were scored for invasion. Data are presented as mean  $\pm$  SD. (C and D)  $Ras^{V12}; M6^{-/-}$  clones in the eye disk stained for common hallmarks of invasive tumors including MMP1 expression and JNK activation. Dashed lines represent outlines of the eye disk. (Scale bar: 100  $\mu$ m.)  $n = 5$ .

As indicated by our clonal screen, M6 mutations are able to synergize with  $Ras^{V12}$  to drive invasion to the ventral nerve cord (VNC) and other more distant tissues as well (Fig. 1A and *SI Appendix, Fig. S2 A and B*).  $Ras^{V12}; M6^{-/-}$  clones displayed the strongest phenotype with invasion to the VNC occurring in

56.6% of larvae examined (Fig. 1B).  $Ras^{V12}; M6^{-/-}$  clones also exhibited some common hallmarks of invasive cancers including MMP1 expression and activation of JNK signaling which is necessary for their growth and invasion (Fig. 1C and D and *SI Appendix, Fig. S2C*) (12). The mammalian homolog of M6, Gpm6a, has been found to be down-regulated in a variety of human cancers of epithelial origin (Oncomine database). Its role as a tumor suppressor that can drive cancerous invasion, as suggested by our screen, remains unexplored. We thus sought to explore how M6 mutations promote the invasion of  $Ras^{V12}$  cells to neighboring tissues.

**Apical Delamination Can Initiate Migration and Invasion of  $Ras^{V12}; M6^{-/-}$  Clones.** To determine how  $Ras^{V12}; M6^{-/-}$  clones are able to depart from their tissue of origin, we utilized the simple morphology of the developing eye disk. The eye disk contains two single-cell epithelial cell layers, the apical surfaces of which face each other to form a common lumen (*SI Appendix, Fig. S4A*). This simple morphology makes it possible to determine if a clone has delaminated from its original tissue as well as to determine if it is located apically or basally relative to the original tissue. Interestingly, while  $Ras^{V12}$  clones remained contiguous with their tissue of origin,  $Ras^{V12}; M6^{-/-}$  clones were often found to be outside of their tissue of origin (Fig. 2A). Around 13% of  $Ras^{V12}; M6^{-/-}$  clones were located apically within the lumen and around 12% of clones were located basally (Fig. 2B).

To determine if either the apically and/or the basally delaminated clones were responsible for the observed invasion into the VNC, we examined fixed tissue samples with the eye discs still connected to the optic lobes of the *Drosophila* central nervous system (and thus the VNC) via the optic stalk (*SI Appendix, Fig. S1A*). As expected based on previous studies documenting basal delamination-induced invasion, we observed basally localized clones invading the optic lobes through the optic stalk (*SI Appendix, Fig. S2C*). Surprisingly, we also found that in 5 of the 13

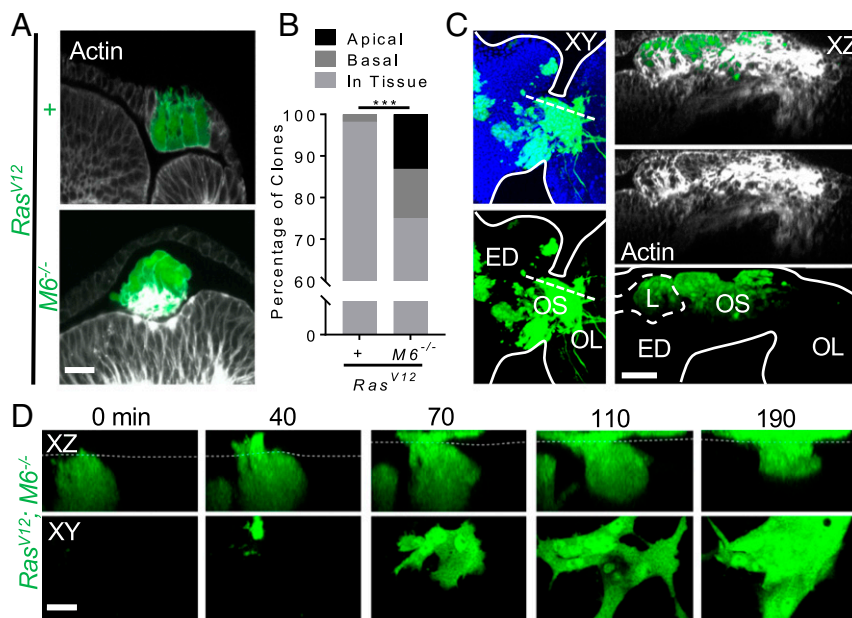


**Fig. 2.**  $Ras^{V12}; M6^{-/-}$  clones delaminate apically from their tissue of origin and are migratory and invasive. (A) Eye discs with  $Ras^{V12}$  and  $Ras^{V12}; M6^{-/-}$  clones stained with phalloidin ( $n = 5$ ). (Scale bar: 10  $\mu$ m.) (B) Quantification of the localization of clones of indicated genotypes. ( $n = 57$  clones for  $Ras^{V12}$  discs, 84 clones for  $Ras^{V12}; M6^{-/-}$ ). Significance was calculated using a  $\chi^2$  test,  $***P < 0.001$ . (C) Fixed tissue samples of  $Ras^{V12}; M6^{-/-}$  clones (GFP) stained with phalloidin (white) in the lumen (L) of the eye discs (ED) still connected to the optic lobes (OL) via the optic stalk (OS) ( $n = 13$  examined). Tissue features were identified with phalloidin staining and anatomical features of the tissue are indicated by white lines. The dashed line in the *Left* panel represents the XZ slice shown in the *Right* panel. (Scale bar: 30  $\mu$ m.) (D)  $Ras^{V12}; M6^{-/-}$  clones were imaged using live ex vivo imaging. Dashed line represents the apical surface of the disk proper as determined through manually positioning each disk before imaging. (*Bottom*) A single z-slice taken with the lumen. (Scale bar: 10  $\mu$ m.) Representative example from  $n = 5$  instances of observed apical migration.

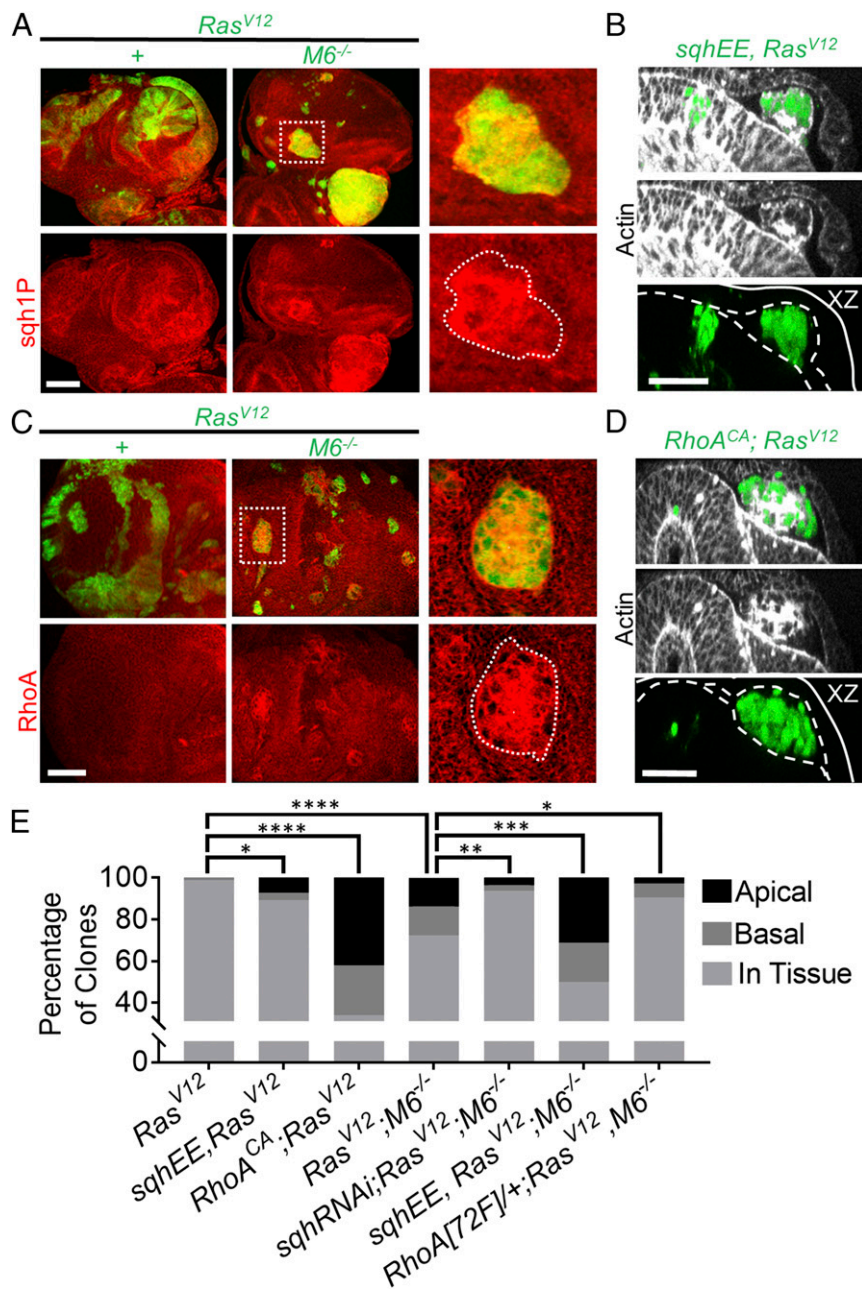


**Fig. 3.** *Ras<sup>V12</sup>; M6<sup>-/-</sup>* clones apically delaminate in a RhoA-activated myosin-dependent manner. (A) *Ras<sup>V12</sup>* and *Ras<sup>V12</sup>; M6<sup>-/-</sup>* eye-disk clones were stained for sqh1P to indicate active myosin. (Scale bar: 50  $\mu$ m.)  $n = 5$ . (Right) Boxed area enlarged. (B) *sqhEE; Ras<sup>V12</sup>* eye-disk clones. Dashed lines represent the apical domains of the peripodial membrane (top dashed line) and the disk proper (bottom dashed line), and the solid line represents the basal surfaces. (Scale bar: 20  $\mu$ m.) (C) *Ras<sup>V12</sup>* and *Ras<sup>V12</sup>; M6<sup>-/-</sup>* eye-disk clones were stained for RhoA ( $n = 5$ ). (Scale bar: 50  $\mu$ m.) (Right) Boxed area enlarged. (D) *RhoA<sup>CA</sup>* was expressed in *Ras<sup>V12</sup>* eye-disk clones and eye discs examined for apical delamination. Dashed lines represent the apical surfaces of the peripodial membrane and disk proper, and the solid line represents the basal surfaces. (Scale bar: 20  $\mu$ m.) (E) Quantification of the localization of clones of indicated genotypes. ( $n = 84$  clones for *Ras<sup>V12</sup>*; 87 clones for *Ras<sup>V12</sup>; M6<sup>-/-</sup>*; 83 clones for *sqhEE, Ras<sup>V12</sup>*; 112 clones for *sqhRNAi; Ras<sup>V12</sup>; M6<sup>-/-</sup>*; 122 clones for *sqhEE, Ras<sup>V12</sup>; M6<sup>-/-</sup>*; 50 clones for *RhoA<sup>CA</sup>, Ras<sup>V12</sup>*; and 106 clones for *RhoA[72F]±; Ras<sup>V12</sup>; M6<sup>-/-</sup>*) Statistical significance was analyzed using  $\chi^2$  analysis with each genotype being compared with the relevant control. \* $P < 0.05$ , \*\* $P < 0.01$ , \*\*\* $P < 0.001$ , and \*\*\*\* $P < 0.0001$ .

the eye discs examined with invasive clones, *Ras<sup>V12</sup>; M6<sup>-/-</sup>* clones that were prominently within the lumen were also able to invade through the optic stalk into the optic lobes (Fig. 2C). Importantly, these clones did not maintain any physical connection to the basal surface of the tissue, confirming that they are completely delaminated from the tissue layers of the eye disk. However, since the eye disk contains a closed lumen, there is also a small group of cells that connects the peripodial membrane to the disk proper at the posterior-most portion of the disk that do

not connect to the basal surface of these layers (orange cells in *SI Appendix, Fig. S2E*). To eliminate the possibility that the observed clones in Fig. 2C could have formed within these cells and merely protruded apically while invading basally in the plane of the tissue, we examined the rate of clone formation in this small group of cells. WT clones (1 clone in 20 discs) and *Ras<sup>V12</sup>* clones (0 clones in 19 discs) formed in these cells at a much lower rate than that observed for the apically located and invasive *Ras<sup>V12</sup>; M6<sup>-/-</sup>* clones (5 clones of 13 discs) ( $P < 0.05$  for WT and  $P < 0.01$

for  $Ras^{V12}$ ). These data show that the invading  $Ras^{V12}; M6^{-/-}$  clones are indeed located within the lumen and are not located within either the tissue layers or the cells that link these layers at the posterior region of the disk.

We further characterized these luminal and invasive cells to understand some of their basic characteristics. The leading edge of these clones can be identified through the presence of actin-rich cell protrusions in the optic lobes (16), suggesting that indeed these luminal clones are migrating toward and into the optic lobes rather than invading back into the lumen (SI Appendix, Fig. S2F). In addition, the basement membrane, as visualized with laminin staining, was unperturbed in these discs, which suggests that these clones are not invading through delaminating apically and subsequent basal invasion and basement membrane degradation (SI Appendix, Fig. S2G). We also explored the dynamics of luminal  $Ras^{V12}; M6^{-/-}$  clone behaviors using live ex vivo imaging of *Drosophila* eye discs. We were able to observe mutant clones that were within the tissue delaminate apically and migrate into and within the lumen, confirming the motility of these clones (Fig. 2D and Movie S1). Taken together, these data implicate apical delamination as a potential initiating step in the process of migration and invasion into surrounding tissues.

We also examined whether loss of M6 in the absence of oncogenic Ras was sufficient to drive the delamination and invasion phenotypes.  $M6^{-/-}$  clones are progressively eliminated during development, but survive when cell death is blocked through expression of the caspase inhibitor p35 (SI Appendix, Fig. S3A and B). We found that loss of M6 alone is sufficient to drive apical delamination of clones when cell death is blocked (SI Appendix, Fig. S3A). Importantly, however, these clones neither overgrow nor invade the VNC (SI Appendix, Fig. S3C), suggesting that apical delamination is not sufficient to drive invasion.

#### Cno-RhoA-MyoII Axis Drives Delamination of $Ras^{V12}; M6^{-/-}$ Clones.

Since our findings indicate that apical delamination can serve as a potential precursor to cancerous invasion, we sought to uncover the mechanism that induced the observed apical delamination in our system. Myosin activation has been shown to be involved in cell extrusion and delamination in a variety of models during both development and cell competition (17, 18). As such, we used an antibody stain against the active monophosphorylated form of *Drosophila* myosin regulatory light chain (Sqh) to detect the levels of myosin activation in our clones. Upon quantification of phosphorylated Sqh staining, we observed a stepwise gradient of myosin activation between clones of different genotypes.  $Ras^{V12}$  clones show an increase in myosin activation over WT clones, and  $Ras^{V12}; M6^{-/-}$  clones show an increase in myosin activation over  $Ras^{V12}$  clones (Fig. 3A and SI Appendix, Fig. S4B). Importantly, every  $Ras^{V12}; M6^{-/-}$  clone within the lumen displayed an increase in sqh1P stain intensity (SI Appendix, Fig. S4B and C).

To determine the necessity of myosin activation for apical delamination, we knocked down *sqh* using RNAi in  $Ras^{V12}; M6^{-/-}$  clones. This resulted in a statistically significant decrease in apically delaminated clones (3.5% of clones delaminated apically) compared with  $Ras^{V12}; M6^{-/-}$  clones alone (Fig. 3E). We further sought to examine the sufficiency of myosin activation for inducing apical delamination-initiated invasion of  $Ras^{V12}$  eye-disk clones. To do this, we expressed a constitutively activated form of Sqh (SqhEE) in  $Ras^{V12}$  clones. This was sufficient to drive apical delamination as it resulted in around 7% of clones delaminating apically, whereas  $Ras^{V12}$  clones alone did not delaminate apically (Fig. 3B and E). In addition to driving apical delamination, myosin activation within  $Ras^{V12}$  clones was sufficient to drive invasion to the VNC (SI Appendix, Fig. S4D). Our findings that  $Ras^{V12}$  clones do not delaminate apically yet still show modest increases in myosin activation suggest that a threshold of myosin activation is required for apical delamination. To test this, we expressed SqhEE in  $Ras^{V12}; M6^{-/-}$  clones to further increase myosin

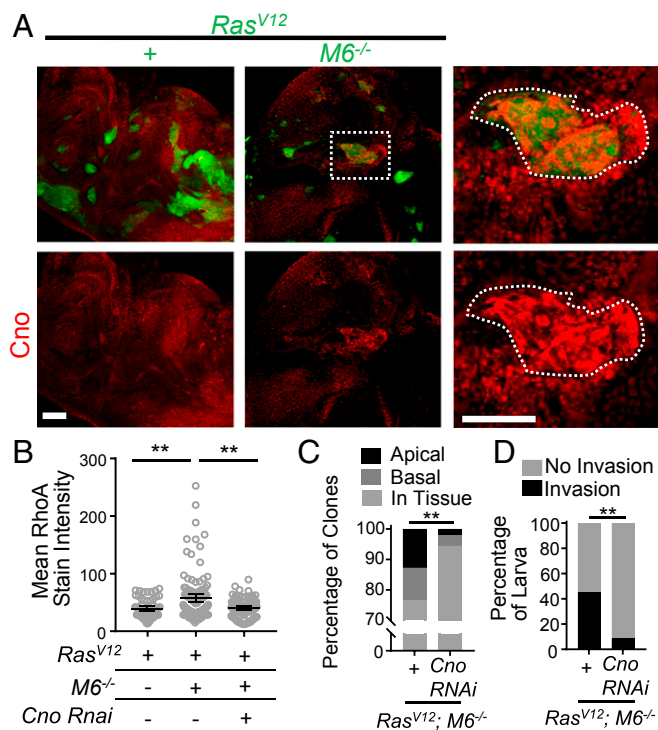


**Fig. 4.** Cno is necessary for RhoA-induced apical delamination and invasion in  $Ras^{V12}; M6^{-/-}$  clones. (A)  $Ras^{V12}$  and  $Ras^{V12}; M6^{-/-}$  eye-disk clones were stained for Cno ( $n = 10$  discs of each genotype). (Scale bar: 50  $\mu\text{m}$ .) (Right) Boxed area enlarged. (Scale bar: Right, 50  $\mu\text{m}$ .) (B) RhoA mean stain intensity was quantified for clones of the indicated genotypes ( $n = 59$   $Ras^{V12}$  clones, 116  $Ras^{V12}; M6^{-/-}$  clones, and 113  $Cno$  RNAi;  $Ras^{V12}; M6^{-/-}$  clones). Significance was calculated using a Mann-Whitney  $U$  test.  $***P < 0.01$ . Data presented as mean with 95% CI. (C) Quantification of the localization of clones of indicated genotypes ( $n = 102$   $Ras^{V12}; M6^{-/-}$  clones and 90  $Cno$  RNAi;  $Ras^{V12}; M6^{-/-}$  clones). Statistical significance was analyzed using  $\chi^2$  analysis.  $***P < 0.01$ . (D) The VNCs from flies of the indicated genotypes were dissected and scored for the presence of GFP+ invasive cells ( $n = 31$   $Ras^{V12}; M6^{-/-}$  clones and 35  $Cno$  RNAi;  $Ras^{V12}; M6^{-/-}$  clones). Significance was calculated using Fisher's exact test.  $***P < 0.01$ .

activation. In line with a myosin activation threshold model, this resulted in an increase in apical (around 31% of clones were located apically) as well as basal (around 19%) delamination (Fig. 3E). Taken together, these findings suggest that ectopic myosin activation is sufficient for inducing apical delamination of  $Ras^{V12}; M6^{-/-}$  clones.

Having uncovered the role of ectopic myosin activation for apical delamination in our system, we searched for the upstream signaling pathways that resulted in the ectopic myosin activation. Rho GTPases are well-studied regulators of the actomyosin network, and ectopic RhoA activity has been shown to synergize with  $Ras^{V12}$  to drive the overgrowth of  $Ras^{V12}$  clones in *Drosophila* (19, 20). In addition to GAP/GEF regulation, RhoA is often regulated by controlling and limiting its localization to specific points in the cell, such as at cell junctions (21). In line with this, we observed that RhoA is mislocalized away from cell boundaries and is enriched throughout the cytoplasm in many  $Ras^{V12}; M6^{-/-}$  clones but not in  $Ras^{V12}$  clones (Fig. 3C). To further validate the involvement of RhoA misregulation in the apical delamination observed in our model, we removed one copy of RhoA in eye discs containing  $Ras^{V12}; M6^{-/-}$  clones and observed a significant suppression of apical delamination (Fig. 3E). We also examined the sufficiency of ectopic RhoA activity to drive apical delamination by expressing a constitutively active form of RhoA (RhoA<sup>CA</sup>) in  $Ras^{V12}$  clones and found that ectopic RhoA activity drove significant delamination and, as previously

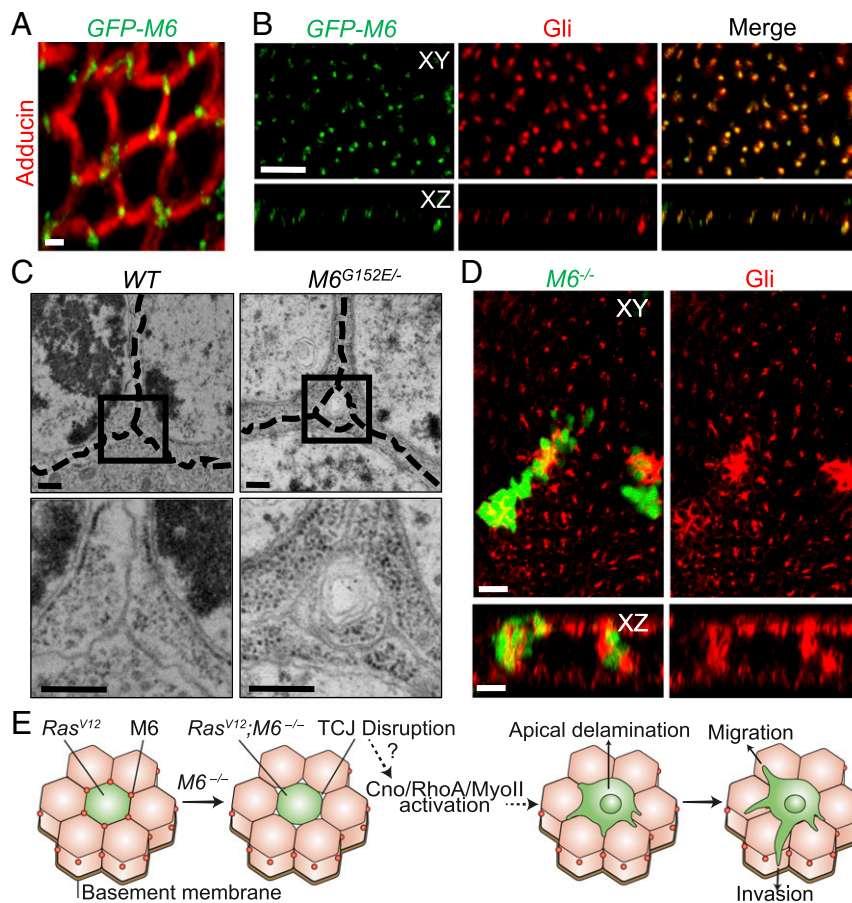


**Fig. 5.** M6 localizes to epithelial tricellular junctions where it is necessary for tricellular junction integrity. (A) Fixed *GFP-M6* eye discs stained with adducin to label membranes ( $n = 10$ ). (Scale bar: 5  $\mu\text{m}$ .) (B) *GFP-M6* eye discs were stained with Gliotactin antibody ( $n = 5$ ). Top represents an XY view, while the Bottom represents an XZ view with the apical surface being located at the top. (Scale bar: 10  $\mu\text{m}$ .) (C) Transmission electron microscopy of WT and *M6<sup>G152E/-</sup>* wing disk TCJs. Dashed lines indicate membranes of adjacent cells ( $n = 3$ ). Boxed region is expanded in the Bottom. (Scale bar: 1  $\mu\text{m}$ .) (D) *M6<sup>-/-</sup>* clones were stained with a Gli antibody ( $n = 5$ ). (Bottom) An XZ view of the clones presented in the Top. (Scale bar: 10  $\mu\text{m}$ .) (E) We present a model of our findings where M6 mutations result in TCJ holes and myosin activation. The activated myosin drives apical delamination, whereby the clones are then able to migrate and invade the surrounding tissues.

reported, it also drove invasion of *Ras<sup>V12</sup>* clones (Fig. 3 D and E and *SI Appendix, Fig. S4E*) (20). Together, these data indicate that misregulation of RhoA activity is necessary to drive apical delamination of *Ras<sup>V12</sup>; M6<sup>-/-</sup>* clones.

We further sought to uncover how M6 functionally connects to RhoA. The protein Cno is a known regulator of RhoA signaling that functions to connect the cytoskeleton to cell junctions (22, 23). In addition, Cno localizes to tricellular junctions during certain developmental stages (24) (the relevance of tricellular junctions is discussed below). Knowing this, we first examined Cno localization in *Ras<sup>V12</sup>; M6<sup>-/-</sup>* clones and found that it was mislocalized and enriched in a manner similar to that seen with RhoA (Fig. 4A). To determine if Cno is necessary for our observed RhoA alterations, we knocked down Cno using RNAi in *Ras<sup>V12</sup>; M6<sup>-/-</sup>* clones. This resulted in a significant decrease in RhoA staining intensity compared with *Ras<sup>V12</sup>; M6<sup>-/-</sup>* clones (Fig. 4B). Furthermore, Cno knockdown in *Ras<sup>V12</sup>; M6<sup>-/-</sup>* clones also inhibited cell delamination and invasion to the VNC (Fig. 4 C and D). Overall, this suggests that Cno is ectopically regulated in *Ras<sup>V12</sup>; M6<sup>-/-</sup>* clones and that these alterations in Cno are at least partially responsible for the observed RhoA-myosin-dependent delamination and invasion.

**M6 Localizes to Tricellular Junctions.** Having discovered the cancerous behaviors of *Ras<sup>V12</sup>; M6<sup>-/-</sup>* clones, we sought to examine the cellular roles of M6 in epithelial tissues. M6 and its mammalian

homolog, GPM6a, have been studied in the past predominately for their roles in the nervous system and the *Drosophila* ovary, and little is known about their roles in imaginal epithelia (14, 25, 26). We used a GFP protein trap fly line (*GFP-M6*) to discover the cellular localization of M6 within imaginal-disk epithelial tissues. This protein trap line does not hamper endogenous M6 function as it is able to rescue the lethality phenotype seen with our *M6* null mutant. Using this line, we found that M6 localizes specifically to tricellular junctions (TCJ) of epithelial tissues and colocalizes with Gliotactin (Gli), a marker of TCJs in *Drosophila* (Fig. 5 A and B and *SI Appendix, Fig. S5A*). TCJ proteins have been shown to play important biological roles in cell division orientation, regulation of cell proliferation, and ionic barrier formation (27–29). In addition, misregulation of human TCJ proteins is known to correlate with a poor prognosis for some cancers (30). It is unclear if mutations in TCJ proteins play a causative role in tumor progression, however, as the results from previous studies have been conflicting (31, 32). Our findings represent a direct causative role for TCJ mutations in driving tumor invasion in vivo.

**M6 Is Necessary for the Structural Integrity of TCJs.** Upon discovery of the unique TCJ localization of M6 in epithelial tissues, and knowing the affects that mutations in other junctional proteins have on junctional integrity (21), we directly asked if M6 mutations affect TCJ integrity. To do this, we examined *M6<sup>G152E/-</sup>* mutant wing imaginal discs by electron microscopy.

Surprisingly, we observed integrity defects specifically at TCJs of M6 mutant tissues as evidenced by small holes at multicellular contacts (Fig. 5C). In WT tissue, the membranes of cells at multicellular contacts were tightly sealed. The bicellular junctions in M6 mutant tissues were indistinguishable from WT when viewed by EM. Lateral EM sections indicated that the holes at multicellular contacts did not extend along the entire basolateral domain but were localized only along the apical portion of the TCJs (SI Appendix, Fig. S5B). In addition to the structural defects observed by EM, we also discovered that M6 is necessary for proper Gli localization as  $M6^{-/-}$  clones show stark Gli mislocalization (Fig. 5D). These results indicate that M6 is necessary for the structural and molecular integrity of TCJs in eye discs.

## Discussion

While bicellular junctions have been well studied for their roles in tissue integrity and signaling, the importance of TCJs has been gradually coming to light in recent years as they have been shown to be key players in ionic barrier formation and maintenance, pathogen spread, and orientation of cell division (27, 28, 33). Here we demonstrate that inactivation of a TCJ protein, M6, disrupts the structural integrity of multicellular contacts and induces apical delamination and invasion of otherwise benign  $Ras^{V12}$  tumors in a manner dependent upon a Cno-RhoA-MyoII axis (Fig. 5E). This study thus provides a causative role for TCJ mutations in driving delamination and invasion in vivo, highlighting the importance of these junctions in tissue integrity and cancer biology.

We also demonstrate a functional link between tricellular junctions and RhoA, which is a known cytoskeletal regulator. This finding adds to recent work that has begun suggesting that TCJs act as centers for cytoskeletal organization (34). It will be interesting to further learn the mechanisms and consequences of functionally linking RhoA and cytoskeletal components to TCJs. Additionally, RhoA is known to affect a variety of proteins and cellular processes in addition to sqh. As such, it is highly possible

that RhoA is inducing apical delamination and invasion through multiple routes in addition to its effects on sqh. Also, since Cno localizes at the adherens junctions, which are apical to M6, it is plausible that M6 only indirectly affects Cno, and thus RhoA, through alterations in epithelial integrity rather than through direct means.

Finally, invasion of cancer cells into surrounding tissues was previously thought to occur only through direct basal delamination and subsequent invasion. Our work shows that apical delamination can also precede migration and invasion to distant tissues. Furthermore, since we did not observe basement membrane degradation in invasive  $Ras^{V12}$ ;  $M6^{-/-}$  clones, the invasion most likely occurs along connected tissues rather than through an apical delamination to the basal penetration route, but further experiments are needed to confirm this hypothesis. Although mammalian anatomy differs markedly from that of the simple architecture of the *Drosophila* imaginal discs, it will be interesting to learn if apical delamination, such as is observed in early stage human breast cancer (9), can also precede invasion in mammalian models. Further investigation into this paradigm of apical delamination-induced invasion could aid our understanding of the mechanisms underlying cancer progression and metastasis.

## Materials and Methods

All *Drosophila* husbandry methods, strains, and procedures have been described before (12) and are further detailed in SI Appendix, Materials and Methods. All imaging was performed according to standard protocols, and all images were analyzed using Imaris Software (Bitplane). Clone localization was determined in a similar manner to that published previously (8, 10). Further details are provided in SI Appendix, Materials and Methods.

**ACKNOWLEDGMENTS.** We thank FlyTrap, the Bloomington Stock Center, the Kyoto *Drosophila* Genome Resource Center, the Developmental Studies Hybridoma Bank, Vanessa Auld, Daisuke Yamamoto, and Robert Ward for providing fly stocks and/or antibodies. We also thank the Howard Hughes Medical Institute for funding this research.

- Eisenhoffer GT, et al. (2012) Crowding induces live cell extrusion to maintain homeostatic cell numbers in epithelia. *Nature* 484:546–549.
- Marinari E, et al. (2012) Live-cell delamination counterbalances epithelial growth to limit tissue overcrowding. *Nature* 484:542–545.
- Shen J, Dahmann C (2005) Extrusion of cells with inappropriate Dpp signaling from *Drosophila* wing disc epithelia. *Science* 307:1789–1790.
- Chaffer CL, Weinberg RA (2011) A perspective on cancer cell metastasis. *Science* 331:1559–1564.
- Slattum GM, Rosenblatt J (2014) Tumour cell invasion: An emerging role for basal epithelial cell extrusion. *Nat Rev Cancer* 14:495–501.
- Kajita M, Fujita Y (2015) EDAC: Epithelial defence against cancer-cell competition between normal and transformed epithelial cells in mammals. *J Biochem* 158:15–23.
- Hendley AM, et al. (2016) p120 catenin suppresses basal epithelial cell extrusion in invasive pancreatic neoplasia. *Cancer Res* 76:3351–3363.
- Tamori Y, Suzuki E, Deng W-M (2016) Epithelial tumors originate in tumor hotspots, a tissue-intrinsic microenvironment. *PLoS Biol* 14:e1002537.
- Leung CT, Brugge JS (2012) Outgrowth of single oncogene-expressing cells from suppressive epithelial environments. *Nature* 482:410–413.
- Vaughen J, Igaki T (2016) Slit- robo repulsive signaling extrudes tumorigenic cells from epithelia. *Dev Cell* 39:683–695.
- Hogan C, et al. (2009) Characterization of the interface between normal and transformed epithelial cells. *Nat Cell Biol* 11:460–467.
- Pagliarini RA, Xu T (2003) A genetic screen in *Drosophila* for metastatic behavior. *Science* 302:1227–1231.
- Dekanty A, Barrio L, Muzzopappa M, Auer H, Milán M (2012) Aneuploidy-induced delaminating cells drive tumorigenesis in *Drosophila* epithelia. *Proc Natl Acad Sci USA* 109:20549–20554.
- Zappia MP, et al. (2012) A role for the membrane protein M6 in the *Drosophila* visual system. *BMC Neurosci* 13:78.
- Wu JS, Luo L (2006) A protocol for mosaic analysis with a repressible cell marker (MARCM) in *Drosophila*. *Nat Protoc* 1:2583–2589.
- Petrie RJ, Yamada KM (2012) At the leading edge of three-dimensional cell migration. *J Cell Sci* 125:5917–5926.
- Grieve AG, Rabouille C (2014) Extracellular cleavage of E-cadherin promotes epithelial cell extrusion. *J Cell Sci* 127:3331–3346.
- Kuipers D, et al. (2014) Epithelial repair is a two-stage process driven first by dying cells and then by their neighbours. *J Cell Sci* 127:1229–1241.
- Kho P, Allan K, Willoughby L, Brumby AM, Richardson HE (2013) In *Drosophila*, RhoGEF2 cooperates with activated Ras in tumorigenesis through a pathway involving Rho1-Rok-Myosin-II and JNK signalling. *Dis Model Mech* 6:661–678.
- Brumby AM, et al. (2011) Identification of novel Ras-cooperating oncogenes in *Drosophila melanogaster*: A RhoGEF/Rho-family/JNK pathway is a central driver of tumorigenesis. *Genetics* 188:105–125.
- Reyes CC, et al. (2014) Anillin regulates cell-cell junction integrity by organizing junctional accumulation of Rho-GTP and actomyosin. *Curr Biol* 24:1263–1270.
- Saito K, et al. (2015) Afadin regulates RhoA/Rho-associated protein kinase signaling to control formation of actin stress fibers in kidney podocytes. *Cytoskeleton (Hoboken)* 72:146–156.
- Majima T, et al. (2013) An adaptor molecule afadin regulates lymphangiogenesis by modulating RhoA activity in the developing mouse embryo. *PLoS One* 8:e68134.
- Sawyer JK, Harris NJ, Slep KC, Gaul U, Peifer M (2009) The *Drosophila* afadin homologue Cnape regulates linkage of the actin cytoskeleton to adherens junctions during apical constriction. *J Cell Biol* 186:57–73.
- Michibata H, et al. (2009) Human GPM6A is associated with differentiation and neuronal migration of neurons derived from human embryonic stem cells. *Stem Cells Dev* 18:629–639.
- Scorticati C, Formoso K, Frasch AC (2011) Neuronal glycoprotein M6a induces filopodia formation via association with cholesterol-rich lipid rafts. *J Neurochem* 119:521–531.
- Riazuddin S, et al. (2006) Tricellulin is a tight-junction protein necessary for hearing. *Am J Hum Genet* 79:1040–1051.
- Bosveld F, et al. (2016) Epithelial tricellular junctions act as interphase cell shape sensors to orient mitosis. *Nature* 530:495–498, and erratum (2016) 534:138.
- Schulte J, Tepass U, Auld VJ (2003) Gliotactin, a novel marker of tricellular junctions, is necessary for septate junction development in *Drosophila*. *J Cell Biol* 161:991–1000.
- Somorácz Á, et al. (2014) Tricellulin expression and its prognostic significance in primary liver carcinomas. *Pathol Oncol Res* 20:755–764.
- Czulkies BA, et al. (2017) Loss of LSR affects epithelial barrier integrity and tumor xenograft growth of CaCo-2 cells. *Oncotarget* 8:37009–37022.
- Shimada H, et al. (2016) The roles of tricellular tight junction protein lipolysis-stimulated lipoprotein receptor in malignancy of human endometrial cancer cells. *Oncotarget* 7:27735–27752.
- Fukumatsu M, et al. (2012) Shigella targets epithelial tricellular junctions and uses a noncanonical clathrin-dependent endocytic pathway to spread between cells. *Cell Host Microbe* 11:325–336.
- Choi W, et al. (2016) Remodeling the zonula adherens in response to tension and the role of afadin in this response. *J Cell Biol* 213:243–260.